Computational and Theoretical Chemistry 990 (2012) 126–131

Contents lists available at SciVerse ScienceDirect

Computational and Theoretical Chemistry

journal homepage: www.elsevier.com/locate/comptc

Energy dissipation channels in the adsorption of N on Ag(1 1 1)

L. Martin-Gondre [a,b,*], G.A. Bocan [c], M. Alducin [a,b], J.I. Juaristi [a,b,d], R. Díez Muiño [a,b]

[a] Centro de Física de Materiales CFM/MPC (CSIC-UPV/EHU), San Sebastián, Spain
[b] Donostia International Physics Center – DIPC, San Sebastián, Spain
[c] CONICET and Centro Atómico Bariloche (CNEA), Av. Bustillo 9500, 8400 S.C. de Bariloche, Argentina
[d] Departamento de Física de Materiales, Facultad de Químicas, UPV/EHU, San Sebastián, Spain

ARTICLE INFO

Article history:
Received 18 November 2011
Received in revised form 19 January 2012
Accepted 10 March 2012
Available online 18 March 2012

Keywords:
Gas/surface dynamics
Non-adiabatic effects
Density functional theory

ABSTRACT

We theoretically study the competition between different energy dissipation channels in the adsorption of N atoms on Ag(1 1 1) surfaces. The three-dimensional potential energy surface that describes the interaction between the N atoms and the metal surface is built from density functional theory calculations. Classical dynamics simulations are subsequently performed to evaluate the adsorption probabilities. The contribution of electron–hole pairs excited in the surface during the adsorption process is included in the simulation by an electronic friction coefficient. Phonon excitations are also considered through the Generalized Langevin Oscillator model. We show that the role of the two channels during the adsorption dynamics is very different: phonons are responsible for determining the adsorption probability but electronic excitations are relevant at a later stage to fix the N atoms to the adsorption positions. We conclude that a theoretical model that intrinsically combines both energy dissipation channels is necessary to properly describe the full dynamics of the process.

1. Introduction

Understanding the interaction of reactive thermal and hyperthermal gas molecules and atoms with metal surfaces has long been a central issue of surface science. These elementary reactive processes are dynamical in nature. Their theoretical study requires thus a precise description of the interaction between atomic and molecular species and the surface, as well as a proper account of the dynamical aspects of the process. In the last decade, methodological advance and highly improved computational capabilities have helped to provide valuable insight into these issues. State-of-the-art theoretical calculations are based nowadays on multidimensional potential energy surfaces (PESs) obtained from first-principles [1]. Dynamics is subsequently introduced by classical or quantum methods. This scheme relies on the validity of the adiabatic approximation in which the total energy of the system is obtained at each time step as that of the ground state. By definition, dissipation of energy to electronic excitations and/or lattice vibrations is neglected in the adiabatic approximation.

Nevertheless, there is always some degree of energy transfer between the incident species and the metal surface. Excitation of electron–hole pairs and energy exchange with phonons are, in general, the most prevalent mechanisms. The question to answer is whether this energy transfer is relevant or not for each particular process under scrutiny. When experimental results and adiabatic calculations are at variance, the difference is often attributed to the neglect of energy loss channels [2], even if the constraints imposed by a reduced dimensionality approximation [3] or the inherent limitations of DFT [4–6] are better grounded arguments.

Concerning electronic excitations, there is ample experimental evidence showing that they do arise in gas/surface experiments [7–10]. Different theoretical models have been thus developed to include this energy dissipation channel [11–15]. Among them, a good compromise between accuracy of results and simplicity of implementation is offered by the local density friction coefficient approximation (LDFA) [15], as shown in Ref. [16]. Within this model, electron–hole pair excitations have been shown to be of minor importance in the dissociation of diatomic molecules on metal surfaces [15], in consistency with previous more qualitative studies [17].

Theoretical activity has been also broad [18–20] in the study of the energy exchange between incident atoms and molecules and the surface lattice. Semiclassical approximations, for instance, in which the gas/surface interaction are modeled in a simplified way have been extensively used [19,21]. This approach has proven to be quite successful for understanding the scattering and energy exchange of non-reactive rare gas atoms [22]. For the scattering of reactive molecules, the model has been also applied and valuable information has been obtained [23]. Nevertheless and for reactive species, the complexity of the interaction prevents the use of such

* Corresponding author at: Centro de Física de Materiales CFM/MPC (CSIC-UPV/EHU), San Sebastián, Spain.
E-mail address: ludovic_martin@ehu.es (L. Martin-Gondre).

2210-271X/$ - see front matter © 2012 Elsevier B.V. All rights reserved.
http://dx.doi.org/10.1016/j.comptc.2012.03.009

simplified descriptions of the molecule-surface potential for quantitative calculations of the reactive and non-reactive rates. In these cases, a more accurate treatment of the interaction is necessary, at least at the level of DFT. In this respect, the Generalized Langevin Oscillator model (GLO) [18] is a valuable tool to incorporate energy exchange with the lattice phonons on top of a multidimensional ab initio PES [24,25].

A reactive process that clearly requires energy transfer to the surface is adsorption. Atoms and molecules incident on metal surfaces and eventually adsorbed must make a transfer of their initial kinetic energy to other channels. In the particular case of atoms that become attached to a metal surface, the dissipative channels are both electronic excitations and phonons. The theoretical study of such processes thus necessitates the inclusion of both dissipative mechanisms in the dynamics. Only recently, a description of the non-reactive scattering processes of atoms and molecules at metal surfaces, using a full-dimensional *ab initio* PES and including both dissipation channels, has been achieved [26]. This theoretical model is particularly appropriate for the description of the adsorption process on metal surfaces.

In the following, we study in detail the adsorption process of N atoms on the Ag(1 1 1) surface. Ueta et al. [27] recently measured the energy loss of N atoms scattered from a clean Ag(1 1 1) surface. They also analyzed the scattering of thermal and hyperthermal Nitrogen from a surface in which N atoms are already adsorbed [28]. For both N atoms and N_2 molecules incident on the N-covered surface, the angle-resolved intensity and final energy curves are very similar to those from the bare surface. For further understanding of these findings we think it is helpful to gain some insight about the dynamics of the adsorption process. Furthermore, we will investigate which is the role of the different energy dissipation channels in the adsorption process, as well as the time-scales in which each one of them act more efficiently. We will show that a theoretical model that intrinsically combines both electron and phonon excitations is necessary to properly describe the full dynamics.

2. Theory

2.1. Potential energy surface

The interaction energy between the N atom and the Ag(1 1 1) surface is obtained from density functional theory (DFT) calculations and used to build a three-dimensional (3D) potential energy surface (PES). Details of the PES calculation can be found in Ref. [29] and are only summarized here. The PES is constructed from a grid of 615 DFT points, corresponding to different positions (X, Y, Z) of the N atom in front of the Ag(1 1 1) surface (Fig. 1). The grid is made of 41 equidistant Z points for each of the 15 (X, Y) sites considered within the unit cell. The N atom (X, Y) positions are selected following symmetry-driven arguments. DFT energy calculations make use of the VASP code [30]. The exchange–correlation energy is calculated within the generalized gradient approximation (GGA) and using Perdew–Wang parametrization [31].

A five-layer slab is used to represent the Ag(1 1 1) surface. The Ag lattice constant, obtained from a bulk calculation, is $a = 4.17$ Å. A (2×2) cell in the plane parallel to the surface is considered, which corresponds to an atomic coverage of 0.25. According to our DFT calculations, geometry corrections due to surface relaxation are very minor. Due to the open-shell nature of the N atom $(1s^2 2s^2 2p^3)$, spin-polarized calculations are required to describe the interaction.

Once the grid of DFT points is built, a numerical interpolation is performed to obtain the value of the interaction energy at any given position of the N atom. The corrugation-reducing procedure [32] is used for this interpolation. The accuracy of the 3D PES is checked by comparing the interpolated values to calculated DFT points not included in the interpolation procedure. Typical differences are found to be lower than 5 meV.

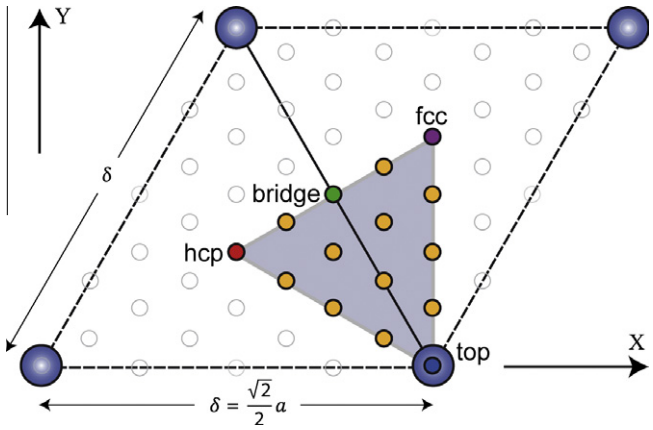

Fig. 1. Geometry of the Ag(1 1 1) surface unit cell. DFT energy calculations have been performed for the 15 sites contained in the shaded area (irreducible unit cell) and marked by a circle.

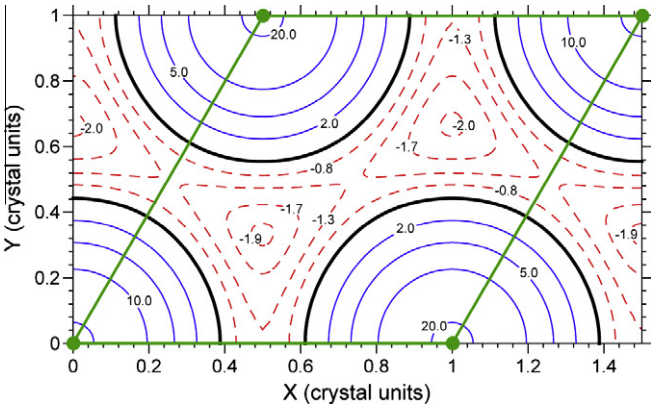

Fig. 2. Contour plot of (X, Y) 2D-cuts of the N/Ag(1 1 1) PES for $Z = 1.20$ Å. X and Y coordinates are given in units of δ and $\sqrt{3/2}\delta$ respectively (see Fig. 1). The black thick solid line corresponds to zero potential energies. Blue thin solid (red dashed) contour lines correspond to positive (negative) values of potential energy (eV). The unit cell is represented by green lines. (For interpretation of the references to color in this figure legend, the reader is referred to the web version of this article.)

A contour plot of (X, Y) 2D-cuts is shown in Fig. 2 for a Z value of 1.20 Å where the deepest adsorption well is observed. This minimum is obtained over the hollow fcc site with an energy of −2.03 eV whereas this energy is of −1.92 eV over the hollow hcp site. At this height above the surface, the presence of the Ag atoms makes the regions around the top sites very repulsive. Therefore, the adsorption process can only occur at the vicinity of the two hollow sites.

2.2. Dynamics and energy dissipation channels

The dynamic interaction between the N atoms and the Ag(1 1 1) surface is studied by means of classical trajectory calculations. A conventional Monte-Carlo procedure is used to sample the initial (X, Y) values over the unit cell. Each trajectory starts at $Z_0 = 6.5$ Å from the surface, where the interaction energy between atom and surface is negligible. Trajectories are propagated in time up to tens of picoseconds. We checked that this integration time

was enough to establish all the possible events (reflection and adsorption). N atoms are considered as reflected when they reach the initial distance Z_0 with a perpendicular component of the velocity opposite in sign to the initial one. N atoms are considered as adsorbed on the Ag(1 1 1) whenever they are not reflected at the end of the trajectory and attain negative values of their total energy E^T. Results shown in this work are typically obtained using 5000 trajectories per incidence angle and energy.

Adsorption of the N atoms on the Ag(1 1 1) surface requires the dissipation of its initial kinetic energy. The initial energy of the N atoms is mostly released through two dissipation channels: electronic excitations and lattice vibrations. Both mechanisms are included into the multidimensional classical trajectory simulations using a combined LDFA + GLO model that is explained in the following. The classical equation of motion for the N atoms incident on the surface reads:

$$\frac{d^2\mathbf{r}_i}{dt^2} = -\frac{1}{m_i}\nabla_i V(\mathbf{r}_i - \mathbf{r}_s) - \frac{1}{m_i}\,\eta(\mathbf{r}_i - \mathbf{r}_s)\frac{d\mathbf{r}_i}{dt}, \tag{1}$$

where m_i and $\mathbf{r}_i$ are the mass and vector position of the gas atom i and $\mathbf{r}_s$ refers to the surface coordinates. The first term on the right hand side is the adiabatic force obtained from the ab initio three-dimensional potential energy surface. The second term on the right hand side consists of a dissipative force that accounts for electron–hole pair excitations. The friction coefficient η is that of the same atom i moving in an homogeneous free electron gas with electronic density equal to that of the surface at the position at which the atom is placed.

The surface motion is represented in terms of a three-dimensional harmonic oscillator with coordinates $\mathbf{r}_s$. In order to consider the coupling and energy-exchange of the surface with the bulk, an additional three-dimensional ghost oscillator is coupled to the surface oscillator. The latter is subject to friction and random forces related to each other through the second fluctuation–dissipation theorem. The ghost particles allow us to represent the bulk of the solid as a thermal bath at the chosen temperature (see Refs. [24–26] for a practical implementation).

3. Dynamical studies of the adsorption process

3.1. Adsorption probability

As mentioned above, classical trajectory calculations have been performed for N atoms impinging on the Ag(1 1 1) surface. For all the calculations considered in this work, no absorption process has been observed. Only adsorption or reflection take place. In the following, we will focus on the first of these processes.

In order to evaluate the role played by the different energy dissipation channels in the adsorption mechanism, three kinds of classical dynamics simulations have been carried out: (i) using the LDFA model to include electronic excitations, (ii) using the GLO model to describe the motion of surface atoms, (iii) including both electron–hole pair excitations and lattice vibration in the LDFA + GLO model. The adsorption probability arising from these three simulations is plotted in Fig. 3 as a function of the incident energy E_i^T. In all cases, the adsorption probability decreases monotonously with increasing E_i^T. At 0.1 eV, the adsorption probability is close to unity, in conformity with the PES topology where no energy barrier is observed for the incoming atom. The N atom is then able to approach the surface and exchange energy through electron–hole pair excitations or lattice vibrations. As the initial kinetic energy is only 0.1 eV, a small energy loss through these energy dissipation channels is enough to trap the atoms at the surface. When the incident energy increases, the energy loss starts to be uneffective to prevent the atom reflection. This leads to a decrease of the adsorption probability.

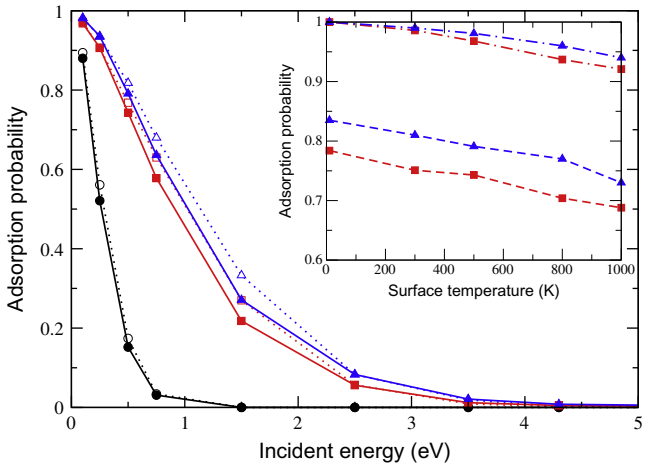

Fig. 3. Adsorption probability as a function of the initial kinetic energy E_i^T for N atoms impinging on Ag(1 1 1). Black circles are the results obtained with the LDFA model, red squares with the GLO model, and blue triangles with LDFA + GLO. The incidence angle is 40° (60°) for the filled symbols/full line (open symbols/dotted line). Surface temperature is 500 K. The inset shows the adsorption probability as a function of surface temperature for two incidence energies: 0.1 eV (dash-dotted line) and 0.5 eV (dashed line) and for an incidence angle of 40°. Red squares and blue triangles are defined as before. (For interpretation of the references to color in this figure legend, the reader is referred to the web version of this article.)

For these higher energies, the adsorption probability given by the LDFA model is always much smaller than the ones obtained with GLO and LDFA + GLO. Moreover, at 1.5 eV there is no adsorption within the LDFA whereas a few atoms can be still adsorbed up to energies of 4 eV when phonon excitations are included. Consequently, the adsorption probability is mainly determined by energy exchange with the lattice and electronic excitations only represent a minor effect as it was already observed for the dissociation probability of diatomic molecules over metallic surfaces [15,33].

The influence of parameters such as the incidence angle Θ_i measured from surface normal and surface temperature T_S is also shown in Fig. 3. When Θ_i increases from 40° (solid lines) to 60° (dotted lines), the adsorption probability is slightly enhanced but the global behavior remains unchanged. This enhancement comes from the decrease of the initial perpendicular energy that decreases the energy loss required to observe a trapping effect. Notwithstanding, a detailed analysis of the full range of incidence angle (from 0° to 80°) shows that the role of Θ_i for adsorption is small.

The influence of T_S is studied in the inset of Fig. 3. These curves show a slight decrease (maximum difference is 0.1 for $E_i^T = 0.5$ eV) of the adsorption probability with the increase of the surface temperature for GLO and for LDFA + GLO as well. The kinetic energy ($k_B T_S$) involved in surface motion for $T_S = 10$, 1000 K is about 0.9 meV and 90 meV, respectively. Thus, even for the highest T_S considered in this work ($T_S = 1000$ K), the initial kinetic energy of the N atoms is always higher. Hence, the N atoms are initially hot compared with the surface. Therefore, on average the N atoms will transfer energy to the surface. This energy balance promotes the trapping of atoms and enhances the adsorption probability. When we compare the lowest and highest T_S, we observe a small temperature dependence as the trapping effect decreases when T_S increases. In the following, since neither the incidence angle nor the surface temperature significantly impact the adsorption probability values, the study will focus on the results obtained for $\Theta_i = 40°$ and $T_S = 500$ K.

The initial and final (X, Y) distributions of N atoms that undergo adsorption is presented in Fig. 4. Except for the LDFA case where the adsorption is not possible for initial positions close to the top sites, for the two others cases, all initial coordinates over the unit cell can lead to adsorption at $E_i^T = 0.1$ eV. In order to understand this result, we briefly survey the dynamics calculations without including any of the energy dissipation channels. In that case, no adsorption is observed after an integration time of 10 ps as no energy loss by the incoming atom is included. Nevertheless, the reflection process is not at all a direct process since on average the atoms are reflected after 3 ps with an average number of rebounds $N_r = 11$. This means that even if the atoms have enough energy to escape from the surface, they spend a relatively large time bouncing at the surface. This process, often called 'dynamic trapping' and already studied for the scattering of atoms over metallic surfaces [34], is caused by the surface corrugation that promotes the energy transfer from motion normal to the surface to motion parallel to the surface and prevents a fast reflection mechanism.

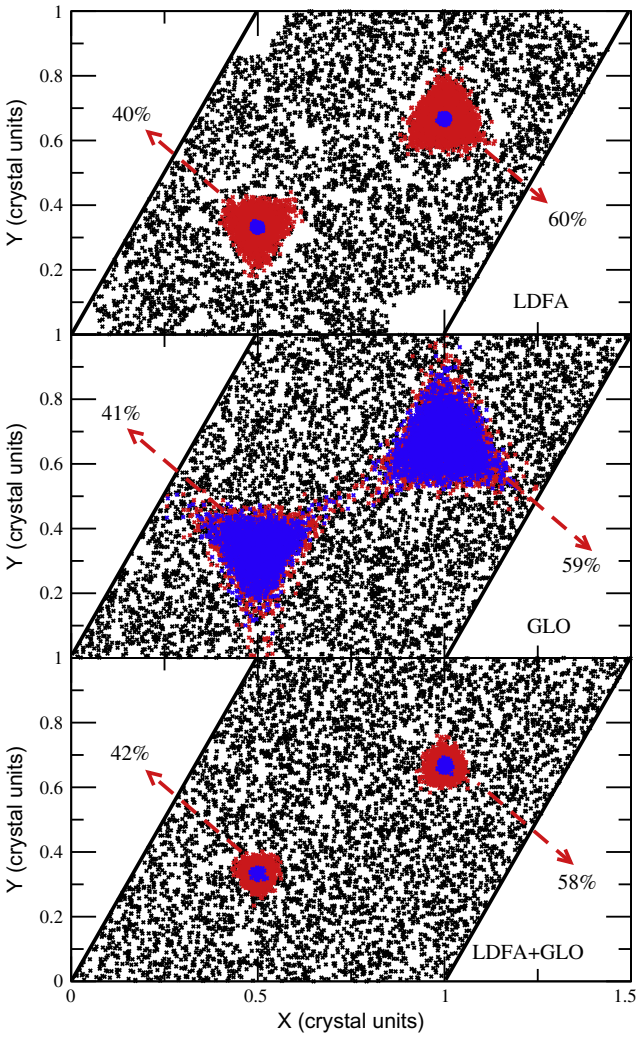

Fig. 4. Initial and final (X, Y) distribution of N atoms over the surface unit cell for an impact energy of 0.1 eV and an incidence angle of 40°. X and Y coordinates are given in the same units as in Fig. 2. Black spots correspond to the initial position of N atoms that become eventually adsorbed. The distributions in red (blue) correspond to the final atomic positions after an integration time of 10 (20) ps. The percentage of atoms adsorbed at the fcc and hcp sites is also indicated. For clarity, all points have been merged into one elementary cell. Surface temperature is 500 K. (For interpretation of the references to color in this figure legend, the reader is referred to the web version of this article.)

Therefore, whatever the initial position of the atoms is, when energy dissipation is included, trapping is so efficient that the trapped atoms can explore the surface until they reach the adsorption wells. It is worth noting that trapping dynamics is efficient at low energies. When initial kinetic energy increases, the energy transfer to parallel motion becomes a minor effect. The energy loss necessary for the trapping of N atoms is then basically due to the energy transfer to phonons. The difference observed for the LDFA calculations is due to a slower energy exchange with electron–hole pair excitations as we will see in the next section. Indeed, among the reflected atoms (≈10% of the total number of atoms), all of them are reflected on the repulsive part of the potential (especially on the top repulsive wall) in a very short time (≈1 ps) for which the energy exchange through electronic excitations is not very significant yet.

Regarding the final (X, Y) distributions, N adsorption occurs on the two hollow sites, hcp and fcc (Fig. 1), in agreement with the PES topology (Fig. 2). Nevertheless, the (X, Y) distribution is quite different depending on the model used. At $t = 10$ ps, the GLO model gives a distribution quite broad compared to the one obtained with the LDFA model. The distribution with LDFA + GLO is narrower. At $t = 20$ ps, the effect of electronic friction is clearly observed since the final distribution of adsorbed atoms is much more localized at the well positions. This is not observed when phonons are included: the atoms are still present in a large region around the hollow sites. These results indicate that electronic excitations play a dominat role in the accommodation of the atoms on the adsorption wells, despite the adsorption probability is ruled by the phonon excitations as shown in Fig. 3. It is worth noting that the adsorption process is more probable on the fcc site (≈60%) than on the hcp site (≈40%). The stronger attraction around the fcc site (Fig. 2) with a deepest well (−2.03 eV) can account for this result.

We have performed a similar analysis of the (X, Y) distributions for $E_i^T = 0.5$ eV and obtained conclusions alike.

3.2. Energy dissipation

A more comprehensive analysis can be done by studying the energy dissipation process for the different simulations. Fig. 5 presents the energy loss distribution ΔE at $E_i^T = 0.1$ eV for two integration times (10 and 20 ps). ΔE is obtained as the difference

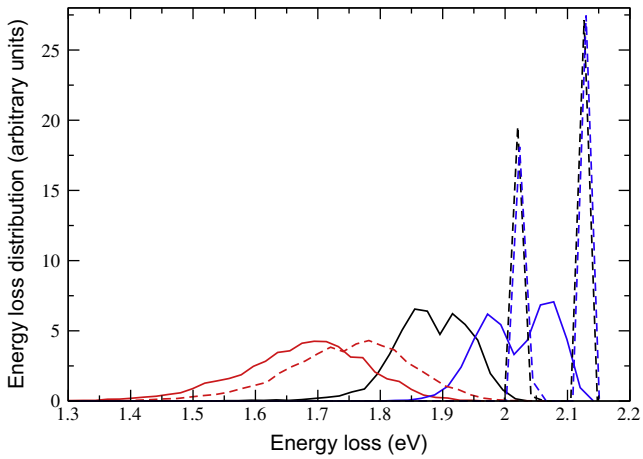

Fig. 5. Energy loss distribution $\left(\Delta E = E_i^T - E_f^T\right)$ of N adsorbed atoms obtained for an initial kinetic energy $E_i^T = 0.1$ eV and an incidence angle of 40°. The results are represented by black lines (LDFA), red lines (GLO) and blue lines (LDFA + GLO) using two integration times: 10 ps (solid lines) and 20 ps (dashed lines). The distributions are normalized to unit area. Surface temperature is 500 K. (For interpretation of the references to color in this figure legend, the reader is referred to the web version of this article.)

between the total initial E_i^T and total final energy E_f^T of the N atom $\left(\Delta E = E_i^T - E_f^T\right)$. Note that E_f^T refers to the kinetic energy E_f^K of the N atom plus the atom/surface potential energy $V\left(E_f^T = E_f^K + V\right)$. As stated in Section 2.1, the minimum adsorption energy is −2.03 eV at the fcc site. Consequently, the maximum energy loss that can be observed for $E_i^T = 0.1$ eV is $\Delta E = 2.13$ eV.

At $t = 10$ ps, significant differences between the three models appear. A broad distribution is obtained within the GLO model reflecting the fact that adsorbed atoms are dispersed around the hollow sites as shown in Fig. 4. Moreover, the maximum of energy that can be lost is about 1.9 eV meaning that no atoms are really sticked at the well positions. With electron–hole pair excitations (with and without phonons), the distribution is narrower and closer to the maximum energy loss, especially when phonons excitations are included. This is linked to the final (X, Y) positions of the N atoms. Fig. 4 shows that they are localized around the wells position for these two models. It follows that the atoms become more strongly adsorbed when electronic excitations are taken into account. This is an important result because even if the adsorption probability is mainly influenced by the energy dissipation through phonons (Fig. 3), the full dynamics and especially the final state of adsorbed atoms shows a completely different picture when electron–hole pair excitations are taken into account.

It is interesting to note that, when electronic excitations are included, the ΔE distributions can be decomposed into two components. The first component, for smaller energy loss, corresponds to the adsorption on the hcp site. The second component corresponds to the adsorption on the fcc site, in agreement with the difference in adsorption energies for the two hollow sites. This double peak is even more distinct when electron and phonon excitations are combined due to a stronger stabilization of the adsorbed atoms. At $t = 20$ ps, a slight increase of the energy loss is observed with the GLO model but still no atoms appear to be really sticked after this long integration time even if it is unlikely that they can escape the attraction of the adsorption wells. In contrast, when electronic friction is included, the two components displayed at $t = 10$ ps are now completely separated and represented by a sharp distribution. After 20 ps, the N atoms are really adsorbed at the bottom of the energy wells since the two peaks correspond to an energy loss of $\Delta E \simeq 2.1$ eV for the fcc site and of $\Delta E \simeq 2.0$ eV for the hcp site in agreement with the depth of the wells. The intensity of the peaks shows the ratio of adsorbed atoms in each of the hollow sites, in correspondence with the percentage given in Fig. 4.

The final position of the adsorbed atoms and the energy loss study show that the electron–hole pair mechanism permits a more stable adsorption of N atoms on the Ag(1 1 1) surface. But, in contrast, the adsorption probability is mostly determined by phonon excitations. We unravel these effects by studying the evolution of the total energy of N atoms E^T during the dynamics, as showed in Fig. 6. For an impact energy of 0.1 eV, the energy dissipation as a function of time presents a very different behavior depending on the models. With the LDFA model, E^T decreases slowly and continuously to reach a full energy dissipation (≈ -2 eV) at 14 ps. Thus, the energy loss due to electronic excitations is effective after the first collisions with the surface due to the value of the friction coefficient η, which is higher close to the surface. On the other hand, the energy dissipation within the GLO model goes down very rapidly until 3 ps and then decreases very slowly during the remaining 17 ps (from −1.45 eV to −1.69 eV). In that case, the mechanism that controls the energy loss is linked to the efficiency of binary-like collisions with the surface atoms. At the beginning of the dynamics, these collisions are particularly efficient since the kinetic energy acquired by the incoming atom at the adsorption wells can be quite high. After an important energy loss during the first picoseconds, the efficiency of the collisions decreases with the kinetic energy of the atom leading to a very long thermalization process. In fact, the integration time used in this work ($t = 20$ ps) is not long enough to reach an equilibrium Boltzmann distribution. We have checked that a full thermalization would require an integration time of at least 50 ps. When electron and phonon excitations are included, the effect of these two dissipation channels is combined into a fast energy dissipation at the beginning of the dynamics and an almost complete energy dissipation at ≃12 ps. The energy dissipation is not fully achieved because there is still energy exchange between the N atoms and the phonons. Nevertheless, the effect of electronic friction in our model limits this energy transfer leading to a roughly constant total energy E^T. For $E_i^T = 0.75$ eV, the global behavior is similar except that the energy dissipation obtained through phonon excitations is more important during the two first picoseconds to compensate the higher E_i^T. In the LDFA model, the energy is dissipated in a continuous way. This means that longer times are required to dissipate larger initial energies (17 ps for $E_i^T = 0.75$ eV and 14 ps for $E_i^T = 0.1$ eV). This is the reason why we observe a strong decrease of the adsorption probability with increasing E_i^T when only electron–hole pair excitations are included (see Fig. 3).

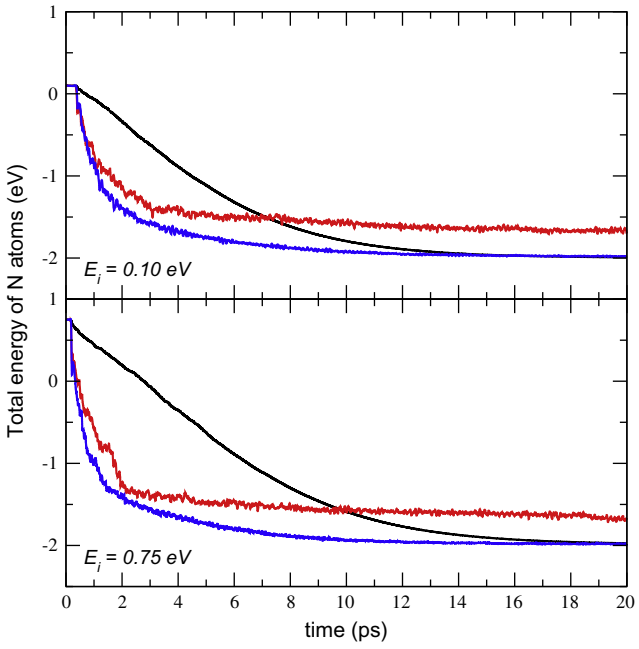

Fig. 6. Evolution of the total energy E^T of N atoms as a function of time representing an average over 10 trajectories and obtained with LDFA (black lines), GLO (red lines) and LDFA + GLO (blue lines). Results are showed for two impact energies and an incidence angle of 40°. Surface temperature is 500 K. (For interpretation of the references to color in this figure legend, the reader is referred to the web version of this article.)

Consequently, these results show that the relevant energy dissipation channels at the beginning and at the end of the dynamics are different. Indeed, the fast energy loss due to phonons during the 2 or 3 first picoseconds of the dynamics will promote the trapping of N atoms, preventing any reflection process. Nevertheless, as the electronic friction acts more continously in time, the final position of the adsorbed atoms is ruled by the latter dissipation channel.

4. Conclusions

The influence of electron and phonon excitations for the adsorption of N on Ag(1 1 1) has been studied. The adsorption probability

appears to be mainly determined by phonon excitations and the inclusion of electron–hole pair excitations only represents a minor effect. Nevertheless, the full dynamical study shows that electronic excitations play a major role in the accommodation features of the adsorbed atoms. In particular, the inclusion of electron–hole pair excitations leads to a more localized adsorption. In conclusion, even it does not clearly appear at first sight, the combination of both electron and phonon excitations is essential to deal with the atomic adsorption process of N on Ag(1 1 1).

Acknowledgments

This work has been supported in part by the Basque Departamento de Educación, Universidades e Investigación, the University of the Basque Country UPV/EHU (Grant No. IT-366-07) and the Spanish Ministerio de Ciencia e Innovación (Grant No. FIS2010-19609-C02-02). Computational resources were provided by the DIPC computing center.

References

[1] A. Gross, in: D.P. Woodruff (Ed.), Surface Dynamics, The Chemical Physics of Solids and Surfaces, vol. 11, Elsevier, Amsterdam, 2003, pp. 1–26.
[2] A.C. Luntz, M. Persson, J. Chem. Phys. 123 (2005) 074704.
[3] C. Díaz, J.K. Vincent, G.P. Krishnamohan, R.A. Olsen, G.J. Kroes, K. Honkala, J.K. Nørskov, Phys. Rev. Lett. 96 (2006) 096102.
[4] G.A. Bocan, R. Díez Muiño, M. Alducin, H.F. Busnengo, A. Salin, J. Chem. Phys. 128 (2008) 154704.
[5] C. Díaz, E. Pijper, R.A. Olsen, H.F. Busnengo, D.J. Auerbach, G.-J. Kroes, Science 326 (2009) 832.
[6] K.R. Geethalakshmi, J.I. Juaristi, R. Díez Muiño, M. Alducin, Phys. Chem. Chem. Phys. 13 (2011) 4357.
[7] B. Gergen, H. Nienhaus, W.H. Weinberg, E.W. McFarland, Science 294 (2001) 2521.
[8] D. Krix, R. Nünthel, H. Nienhaus, Phys. Rev. B 75 (2007) 073410.
[9] J.D. White, J. Chen, D. Matsiev, D.J. Auerbach, A. Wodtke, Nature 433 (2005) 503.
[10] I. Rahinov, R. Cooper, D. Matsiev, C. Bartels, D.J. Auerbach, A.M. Wodtke, Phys. Chem. Chem. Phys. 13 (2011) 12680.
[11] M. Head-Gordon, J.C. Tully, J. Chem. Phys. 103 (1995) 10137.
[12] J.R. Trail, D.M. Bird, M. Persson, S. Holloway, J. Chem. Phys. 119 (2003) 4539.
[13] N. Shenvi, S. Roy, J.C. Tully, Science 326 (2009) 829.
[14] S. Monturet, P. Saalfrank, Phys. Rev. B 82 (2010) 075404.
[15] J.I. Juaristi, M. Alducin, R. Díez Muiño, H.F. Busnengo, A. Salin, Phys. Rev. Lett. 100 (2008) 116102.
[16] J.C. Tremblay, S. Monturet, P. Saalfrank, Phys. Rev. B 81 (2010) 125408.
[17] P. Nieto, E. Pijper, D. Barredo, G. Laurent, R.A. Olsen, E.J. Baerends, G.J. Kroes, D. Farias, Science 312 (2006) 86.
[18] J.C. Tully, J. Chem. Phys. 73 (1980) 1975.
[19] J.R. Manson, Phys. Rev. B 43 (1991) 6924.
[20] M. Dohle, P. Saalfrank, Surf. Sci. 373 (1997) 95.
[21] J.R. Manson, Phys. Rev. B 58 (1998) 2253.
[22] W.W. Hayes, J.R. Manson, Phys. Rev. B 75 (2007) 113408.
[23] H. Ambaye, J.R. Manson, J. Chem. Phys. 125 (2006) 084717.
[24] H.F. Busnengo, W. Dong, A. Salin, Phys. Rev. Lett. 93 (2004) 236103.
[25] H.F. Busnengo, M.A. Di Césare, W. Dong, A. Salin, Phys. Rev. B 72 (2005) 125411.
[26] L. Martin-Gondre, M. Alducin, G.A. Bocan, R. Díez Muiño, J.I. Juaristi, Phys. Rev. Lett. 108 (2012) 096101.
[27] H. Ueta, M.A. Gleeson, A.W. Kleyn, J. Phys. Chem. A 113 (2009) 15092.
[28] H. Ueta, M.A. Gleeson, A.W. Kleyn, J. Chem. Phys. 135 (2011) 074702.
[29] M.S. Gravielle, G.A. Bocan, R. Díez Muiño, Phys. Rev. A 82 (2010) 052904.
[30] G. Kresse, J. Hafner, Phys. Rev. B 47 (1993) 558;
G. Kresse, J. Hafner, Phys. Rev. B 48 (1993) 13115;
G. Kresse, J. Furthmüller, Comput. Mater. Sci. 6 (1996) 15;
G. Kresse, J. Furthmüller, Phys. Rev. B 54 (1996) 11169.
[31] J.P. Perdew, J.A. Chevary, S.H. Vosko, K.A. Jackson, M.R. Pederson, D.J. Singh, C. Fiolhais, Phys. Rev. B 46 (1992) 6671.
[32] H.F. Busnengo, A. Salin, W. Dong, J. Chem. Phys. 112 (2000) 7641.
[33] I. Goikoetxea, J.I. Juaristi, M. Alducin, R. Díez Muiño, J. Phys.: Condens. Matter 21 (2009) 264007.
[34] G. Volpilhac, H.F. Busnengo, W. Dong, A. Salin, Surf. Sci. 544 (2003) 329.